

# Fault-tolerant model predictive control of a wind turbine benchmark

X. Yang\* J.M. Maciejowski\*

\* Cambridge University Engineering Dept., Cambridge CB2 1PZ, UK

## Abstract:

This paper aims to solve the fault tolerant control problem of a wind turbine benchmark. A hierarchical controller with model predictive pre-compensators, a global model predictive controller and a supervisory controller is proposed. In the model predictive pre-compensator, an extended Kalman Filter is designed to estimate the system states and various fault parameters. Based on the estimation, a group of model predictive controllers are designed to compensate the fault effects for each component of the wind turbine. The global MPC is used to schedule the operation of the components and exploit potential system-level redundancies. Extensive simulations of various fault conditions show that the proposed controller has small transients when faults occur and uses smoother and smaller generator torque and pitch angle inputs than the default controller. This paper shows that MPC can be a good candidate for fault tolerant controllers, especially the one with an adaptive internal model combined with a parameter estimation and update mechanism, such as an extended Kalman Filter.

Keywords: fault tolerant control, model predictive control, extended Kalman Filter, wind turbine benchmark

## NOMENCLATURE

$v_w$	wind speed	$\tau_r$	rotor torque
$\tau_g$	generator torque	$\omega_r$	rotor speed
$\omega_g$	generator speed	$\beta$	pitch angle
$P_g$	generator power	$P_r$	rated power
subscript $r$	reference value or rotor variable		
subscript $m$	measurement		

## 1. INTRODUCTION

Wind energy has been utilised for a long time as a renewable energy source. But wind farms are usually located at offshore, desert or mountain regions, where wind energy is abundant but maintenance costs for the wind turbines are high. For economic reasons, fault tolerance capabilities of wind turbines are desirable. Wind turbines exhibit behaviours like wind-generated noise, nonlinear aerodynamics, vibration in the components, etc. In [1], an active fault-tolerant Linear Parameter Varying (LPV) controller is designed by treating the fault parameters as extra scheduling parameters. As an alternative, a passive fault-tolerant LPV controller is designed by viewing the fault as unmeasured parameter variations. In [2], an active fault tolerant approach to wind turbine control based on a fuzzy state observer and a fuzzy controller is implemented, to cope with parametric uncertainties and sensor faults. A benchmark for the fault tolerant control of wind turbine is also proposed in [3], to promote research in this area. This paper address the problems defined in this benchmark.

Model predictive control (MPC) inherently and systematically handles constraints and optimises the control to meet the objectives. Moreover, the implicit fault tolerant

capability of constrained predictive control is discovered and illustrated in [4]. In this paper, a novel active fault tolerant controller for wind turbine is proposed, which adopts MPC as a nominal controller and as the pre-compensators for each component. This controller can fulfil the aim of both performance optimisation and fault compensation.

The following assumptions and simplifications are made. In terms of the wind turbine, the structure is assumed to be rigid and the yaw control is not considered[1]. High-severity faults are not considered, either, as no compensation is needed but to shut down the wind turbine, according to the benchmark definition. The Fault Detection and Isolation (FDI) procedure is assumed to give the fault severity and faulty component information when fault happens, with delays specified in the benchmark.

## 2. DESCRIPTION OF THE BENCHMARK

### 2.1 Wind Turbine Description

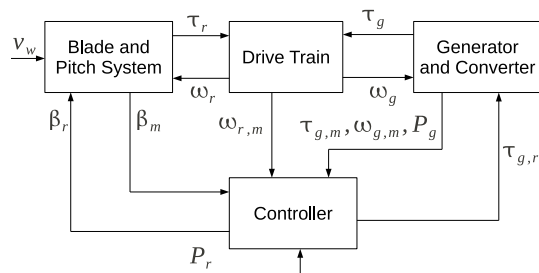


Fig. 1. Block diagram of the wind turbine benchmark[3]

Fig. 1 illustrates the block diagram for the operation of the wind turbine benchmark. A wind turbine mainly consists of the blade and pitch system, the drive train system, the generator and converter, and the controller. Through the aerodynamic forces, blades act as the media for wind power acquisition. The pitch system manipulates the pitch angle of each blade, thus controlling the aerodynamic forces and the power captured. The drive train system connects the rotor shaft (low speed shaft) to the generator shaft (high speed shaft), and transmits the aerodynamic torque from the rotor to the generator. The generator and converter is normally an induction generator equipped with power electronics devices, which produces electricity and modifies its characteristics. The controller is the ‘brain’ for all the above parts and schedules their operation, as well as providing feedback action.

Wind turbine operation is closely related to the wind speed. Four regions can be distinguished, as illustrated in Fig. 2. In Fig. 2,  $v_{min}$  and  $v_{max}$  are the cut-in and cut-out wind speeds, respectively. Region II corresponds to

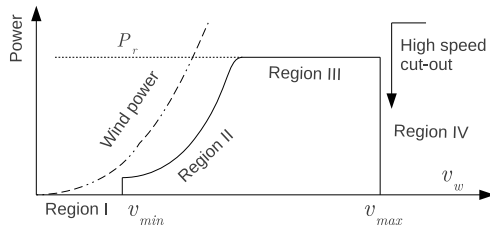


Fig. 2. Steady-state power curve of wind turbine[5, 6]

low wind speed, indicating low wind power. The control objective in this region is to capture the maximum wind power available. Region III corresponds to relatively high wind speed, implying high wind energy. To ensure that the wind turbine works within its limits, the control objective in this region is to operate the wind turbine at the nominal power and release excessive wind energy. The other two regions, I and IV, correspond to extremely low and high wind speeds, in which situations the wind turbine will be shut down for economic or safety reasons.

## 2.2 Fault Scenarios

There are two types of faults in the pitch system: (1) the presence of air in the hydraulic oil (Fault 5b in [3]). This is considered to be a ‘medium severity’ actuator fault. (2) Pump leakage or other pump problems (Fault 5a in [3]). This is considered to be a ‘high severity’ actuator fault. These faults lead to changed dynamics of the system, which can be seen from Fig. 3, which depicts the pitch angle responses to a unit step reference input in nominal and faulty situations. The medium-severity fault causes variation in natural frequency and damping ratio of the pitch system. The variation is parameterised by  $\alpha$ , which is a linear interpolation parameter between the nominal values and the worst case values, as in (1) and (2)[1].

$$\omega_n(t) = [1 - \alpha(t)]\omega_{n,0} + \alpha(t)\omega_{n,2} \quad (1)$$

$$\zeta(t) = [1 - \alpha(t)]\zeta_0 + \alpha(t)\zeta_2 \quad (2)$$

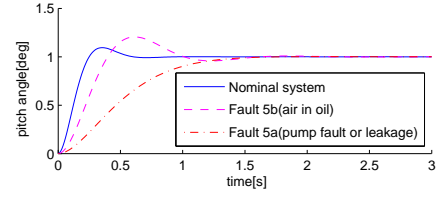


Fig. 3. Comparison of step responses between nominal and faulty cases

where  $\omega_n(t)$  and  $\zeta(t)$  are the natural frequency and damping ratio of the pitch system, respectively. Subscript  $_0$  indicates the nominal values, and  $_2$  the worst case values.

The fault in the drive train system is an increased level of friction. It is characterised by a reduced efficiency, which deviates from its nominal value  $\eta_{dt,0}$  to  $\eta_{dt}$ . By defining the relative efficiency  $\eta_r$  as the ratio of the actual value  $\eta_{dt}$  to the nominal one, the drive train fault can be parameterised by  $\eta_r$  as

$$\eta_{dt} = \eta_{dt,0}\eta_r, \quad \eta_r \in [0, 1] \quad (3)$$

Fig. 4 is the rotor speed response to a step in the rotor torque input, depicting the fault effect on the drive train system.

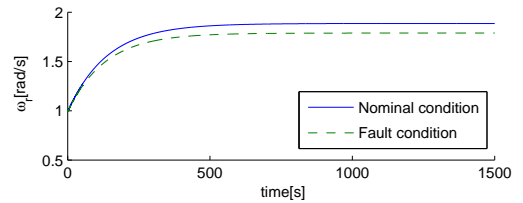


Fig. 4. Comparison of rotor speed output ( $\omega_r$ ) between the nominal and fault conditions

Sensor faults in the benchmark have relatively low severity due to the double redundancy configuration of most sensors. There are two types of sensor faults, constant output and constant gain factor, which can be uniformly represented as

$$y_f = \kappa y_m + \Delta y_m \quad (4)$$

in which  $y_m$  and  $y_f$  are the healthy and faulty measurements, respectively;  $\kappa$  and  $\Delta y_m$  are the two parameters denoting the gain factor and bias. Different combination of the values of  $\kappa$  and  $\Delta y_m$  and the corresponding sensor conditions are listed below.

- (1)  $\Delta y_m = 0$ ,  $\kappa = 1$ , normal condition.
- (2)  $\Delta y_m = 0$ ,  $\kappa \neq 1$ , fault of constant gain factor.
- (3)  $\Delta y_m \neq 0$ ,  $\kappa = 0$ , fault of constant output.

Requirements for fault tolerant controller design[3] are briefly listed as follows.

- (1) Nominal performance under medium and low severity faults.
- (2) Nominal performance with one sensor fault, possibly degraded performance with other faults.
- (3) Small transient during the fault accommodation. Fault accommodation is defined as change in controller parameters or structure to avoid the consequences of a fault[7].
- (4) FDI results could be utilised, but with time delays specified in the benchmark.

### 3. CONTROLLER DESIGN

The general structure of the proposed fault-tolerant model predictive controller is illustrated in Fig. 5 with 3 levels of control action. The supervisory control accepts external information, such as the FDI results, commands from the operators, etc., and manages objectives and constraints of all the lower-level model predictive controllers through the mode control flow. The global model predictive controller functions as a nominal controller for the plant and generates the reference inputs. The model predictive pre-compensators are for the compensation of possible actuator, sensor or system faults in each component of the plant.

One feature of this structure lies in the model predictive pre-compensators, which compensate the fault effects and ‘hide’ them from the global model predictive controller. It decouples the fault compensation task from the nominal controller design. Thus, existing nominal controllers of any form could be utilised. Another feature of this structure is the management and propagation of the objectives and constraints through mode control flow. These objective and constraints can be the nominal ones. But in case of serious faults when the nominal performance cannot be achieved, the objectives could be switched to degraded ones and the constraints can also be updated if necessary. The powerful ‘actuator’ to carry out the objective is the optimisation lying in the global and lower-level model predictive controllers.

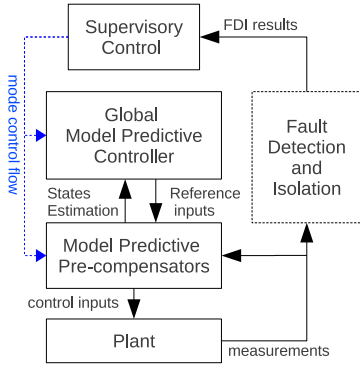


Fig. 5. Structure of the fault-tolerant model predictive controller

#### 3.1 Model predictive pre-compensator

The aim of the model predictive pre-compensator is to compensate the faulty system by an MPC, such that the compensated system has the closest response to the nominal system and the constraints are not violated. A *General fault compensation problem* is posed as: For a system

$$\dot{\mathbf{x}} = \mathbf{A}(\xi_c)\mathbf{x} + \mathbf{B}(\xi_c)\mathbf{u} + \mathbf{w} \quad (5)$$

$$\mathbf{y} = \mathbf{C}\mathbf{x} \quad (6)$$

$$\mathbf{y}_f = \mathbf{g}(\mathbf{y}, \xi_f) + \mathbf{v} \quad (7)$$

and a reference model

$$\dot{\mathbf{x}}_r = \mathbf{A}(\xi_{c0})\mathbf{x}_r + \mathbf{B}(\xi_{c0})\mathbf{u}_r \quad (8)$$

$$\mathbf{y}_r = \mathbf{C}\mathbf{x}_r \quad (9)$$

the *general fault compensation problem* is defined as: Given  $\mathbf{u}_r$ , find  $\mathbf{u}$ , which minimises

$$J = \int_{t_k}^{t_k + N_c \Delta t} (\|\mathbf{x} - \mathbf{x}_r\|_{\mathbf{Q}}^2 + \|\dot{\mathbf{u}}\|_{\mathbf{R}}^2) d\tau \quad (10)$$

In eq. (5) to (7), matrices  $\mathbf{A}$ ,  $\mathbf{B}$  and  $\mathbf{C}$  are in compatible dimensions;  $\xi_c$  and  $\xi_f$  are the system(actuator) and the sensor fault parameters, respectively;  $\mathbf{y}_f$  is the sensor measurement;  $\mathbf{w}$  and  $\mathbf{v}$  are the process noise and the output noise, respectively;  $\mathbf{w} \sim N(\mathbf{0}, \mathbf{Q}_w)$ ,  $\mathbf{v} \sim N(\mathbf{0}, \mathbf{Q}_v)$ ;  $\mathbf{g}(\cdot)$  is a nonlinear function. In eq. (8) to (10),  $\xi_{c0}$  is the nominal value for  $\xi_c$ ;  $t_k$  is the current time;  $\Delta t$  is the control interval;  $N_c$  is the length of the control horizon;  $\mathbf{Q}$  and  $\mathbf{R}$  are weighting matrices.

This problem can be solved in two steps: parameter estimation and MPC design. Assume  $\epsilon_c$  and  $\epsilon_f$  are unknown constants distorted by additive white Gaussian noise  $\mathbf{w}_{\epsilon_c}$  and  $\mathbf{w}_{\epsilon_f}$ . By augmenting both  $\xi_c$  and  $\xi_f$  as extra states and eliminating  $\mathbf{y}$ , eq. (5) to (7) could be written as

$$\dot{\mathbf{x}} = \mathbf{A}(\xi_c)\mathbf{x} + \mathbf{B}(\xi_c)\mathbf{u} + \mathbf{w} \quad (11)$$

$$\dot{\xi}_c = \mathbf{0} + \mathbf{w}_{\xi_c} \quad (12)$$

$$\dot{\xi}_f = \mathbf{0} + \mathbf{w}_{\xi_f} \quad (13)$$

$$\mathbf{y}_f = \mathbf{g}(\mathbf{C}\mathbf{x}, \xi_f) + \mathbf{v} \quad (14)$$

where  $\mathbf{w}_{\xi_c} \sim N(\mathbf{0}, \mathbf{Q}_{\xi_c})$  and  $\mathbf{w}_{\xi_f} \sim N(\mathbf{0}, \mathbf{Q}_{\xi_f})$ .  $\mathbf{w}$ ,  $\mathbf{w}_{\xi_c}$  and  $\mathbf{w}_{\xi_f}$  are assumed to be white and statistically independent. By writing eq. (11) to (14) in a compact form as

$$\dot{\mathbf{x}}_a = \mathbf{f}_a(\mathbf{x}_a, \mathbf{u}) + \mathbf{w}_a \quad (15)$$

$$\mathbf{y}_f = \mathbf{h}(\mathbf{x}_a) + \mathbf{v} \quad (16)$$

in which

$$\mathbf{x}_a = \begin{bmatrix} \mathbf{x} \\ \xi_c \\ \xi_f \end{bmatrix}, \mathbf{f}_a = \begin{bmatrix} \mathbf{A}(\xi_c)\mathbf{x} + \mathbf{B}(\xi_c)\mathbf{u} \\ \mathbf{0} \\ \mathbf{0} \end{bmatrix}, \mathbf{w}_a = \begin{bmatrix} \mathbf{w} \\ \mathbf{w}_{\xi_c} \\ \mathbf{w}_{\xi_f} \end{bmatrix}$$

$$\mathbf{h} = \mathbf{g}(\mathbf{C}\mathbf{x}, \xi_f)$$

and defining

$$\mathbf{Q}_a = \text{diag}(\mathbf{Q}_w, \mathbf{Q}_{\xi_c}, \mathbf{Q}_{\xi_f}), \quad \mathbf{R}_a = \mathbf{R}_v \quad (17)$$

and

$$\mathbf{F} = \left. \frac{\partial \mathbf{f}_a}{\partial \mathbf{x}_a} \right|_{\mathbf{x}_a, \mathbf{u}}, \quad \mathbf{H} = \left. \frac{\partial \mathbf{h}}{\partial \mathbf{x}_a} \right|_{\mathbf{x}_a} \quad (18)$$

, the continuous-time extended Kalman Filter (19) to (21) can be used to estimate the augmented state vector:

$$\dot{\hat{\mathbf{x}}}_a = \mathbf{f}_a(\hat{\mathbf{x}}_a, \mathbf{u}) + \mathbf{K}(\mathbf{y}_f - \mathbf{h}(\hat{\mathbf{x}}_a)) \quad (19)$$

$$\dot{\mathbf{P}} = \mathbf{F}\mathbf{P} + \mathbf{P}\mathbf{F}^T - \mathbf{K}\mathbf{H}\mathbf{P} + \mathbf{Q}_a \quad (20)$$

$$\mathbf{K} = \mathbf{P}\mathbf{H}^T\mathbf{R}_a^{-1} \quad (21)$$

Based on the estimation of the augmented state vector  $\hat{\mathbf{x}}_a$ , an MPC can be designed, which contains an internal reference model and an adaptive internal model, and has the objective function as

$$\int_{t_k}^{t_k + N_c \Delta t} [(\mathbf{x}_d - \mathbf{x}_r)^T \mathbf{Q}(\mathbf{x}_d - \mathbf{x}_r) + \dot{\mathbf{u}}^T \mathbf{R} \dot{\mathbf{u}}] dt \quad (22)$$

in which  $\mathbf{x}_d$  and  $\mathbf{x}_r$  are the states of the internal reference model and the adaptive internal model, respectively. The

MPC solves this general fault compensation problem, as long as the estimation of states and parameters by the extended Kalman Filter is correct.

An illustration of the structure of the model predictive pre-compensator is shown in Fig. 6.

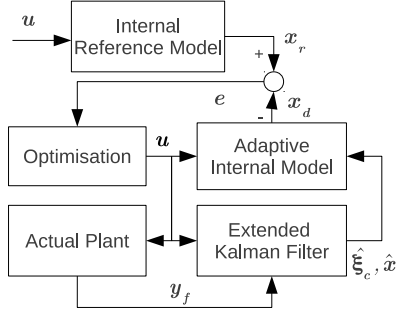


Fig. 6. Structure of the model predictive pre-compensator

For the benchmark problem, two pre-compensators are designed, namely the pitch system pre-compensator and the drive trains system pre-compensator. The system (actuator) fault parameters  $\xi_c$  are chosen to be  $\alpha$  and  $\eta_r$  correspondingly ( See (1) - (3) ). To deal with sensor faults, assume  $\mathbf{y}_f \in \mathbb{R}^p$ ,  $\mathbf{x} \in \mathbb{R}^n$  and double redundancy is available on each output, then

$$\mathbf{y}_f = \mathbf{K}\mathbf{C}\mathbf{x} + \Delta\mathbf{y}_f + \mathbf{v} \quad (23)$$

where  $\mathbf{K} \in \mathbb{R}^{2p \times n}$ ,  $\mathbf{y}_f \in \mathbb{R}^{2p}$  and

$$\mathbf{K} = \begin{bmatrix} \kappa_{1,1} & 0 & \dots & 0 \\ \kappa_{1,2} & 0 & \dots & 0 \\ 0 & \kappa_{2,1} & \dots & 0 \\ 0 & \kappa_{2,2} & \dots & 0 \\ \vdots & \vdots & \ddots & \vdots \\ 0 & 0 & 0 & \kappa_{p,1} \\ 0 & 0 & 0 & \kappa_{p,2} \end{bmatrix} \quad (24)$$

$$\Delta\mathbf{y}_f = [\Delta y_{1,1} \ \Delta y_{1,2} \ \dots \ \Delta y_{p,1} \ \Delta y_{p,2}]^T \quad (25)$$

where  $\kappa_{i,j}$  and  $\Delta y_{i,j}$  ( $i = 1, \dots, p$ ;  $j = 1, 2$ ) are the fixed gain fault and the fixed bias fault parameters on the  $j^{th}$  sensor of the  $i^{th}$  output, respectively.  $\mathbf{K}$  and  $\Delta\mathbf{y}_f$  form the sensor fault parameters  $\xi_f$  in (14). Local observability of the augmented system is essential for state estimation, which can be established by considering  $\xi_c$  and  $\xi_f$  subsequently. Detailed observability results and the corresponding proof can be found in [8]. Results for the benchmark are as follows.

- (1) The origin is not locally observable both for the pitch system and the drive train system.
- (2) The steady state is not observable for the pitch system.
- (3) If two sensors of the same output both suffer from faults of constant output, the pitch system is not observable while the drive train system is still observable with faults on one single output.

### 3.2 Global model predictive controller

The global model predictive controller is a nonlinear MPC with the nominal model of the pitch system, the drive

train system and the nonlinear aerodynamics data as the prediction model. This global MPC takes the states of the pitch system and the drive train system as inputs, which comes from the estimation of the pre-compensators. The outputs: the generator torque  $\tau_{g,r}$  and the pitch angle  $\beta_r$ , are reference values for the pre-compensators. The objective function of the global MPC is

$$J = \int_{t_k}^{t_k + N_c \Delta t} (\mathbf{h} - \mathbf{r})^T \mathbf{Q} (\mathbf{h} - \mathbf{r}) dt \quad (26)$$

where  $\mathbf{h}$  is a vector of penalised variables in all possible working conditions;  $\mathbf{r}$  is a vector of reference values for  $\mathbf{h}$ ;  $\mathbf{Q}$  is a time-varying weighting matrix. For the benchmark problem,

$$\mathbf{h} = \left[ \frac{\omega_r R}{v_w} \ \omega_g \ \beta_r \ \tau_{g,r} \ \dot{\beta}_r \ \dot{\tau}_{g,r} \right]^T \quad (27)$$

$$\mathbf{r} = \left[ \lambda_{opt} \ \omega_{g,nom} \ 0 \ \frac{P_r}{\omega_{g,nom} \eta_g} \ 0 \ 0 \right]^T \quad (28)$$

$$\mathbf{Q} = \begin{cases} \text{diag}(1 \ 0 \ 1 \ 0 \ 0 \ 10^{-10}) & \text{Region II} \\ \text{diag}(0 \ 1 \ 0 \ 1 \ 0.1 \ 0.1) & \text{Region III} \end{cases} \quad (29)$$

### 3.3 Supervisory control

The supervisory control consists of an input interface, internal logic and an output interface. The input interface accepts the operator input and the fault detection and isolation (FDI) results. The operator input allows the operator to interact with lower level controllers, such as manually adjust the constraints or objectives or other necessary human intervention. The FDI input provides fault severity level and fault source information to the control logic. Since the proposed fault-tolerant model predictive controller does not need detailed fault information, no other FDI information is needed. The internal logic manages the switches among different operating modes and the corresponding objectives and constraints, which are transmitted through the output interface to the lower level controllers.

## 4. SIMULATION RESULTS

All the MPC controllers are implemented with the ACADO software toolkit[9].

### 4.1 Fault Compensation Simulation

This part contains a series of simulations to demonstrate the performance of the model predictive pre-compensators. The medium-severity pitch actuator fault, drive train system fault and low-severity sensor faults are covered here. Fig. 7 shows the compensation for the pitch system actuator fault. In Fig. 7a, large overshoot and slowed action occur in the faulty system, while the response of the compensated system is close to the nominal case. Fig. 7b shows how the compensation is achieved. As can be seen, the pre-compensator modifies the reference input. When the step occurs, the pre-compensator first increases the magnitude of the input in order to increase the speed of the response. It then decreases the magnitude in order to suppress the overshoot.

Fig. 8 shows the compensation for the drive train system fault, with input of a constant 800000 N·m rotor torque

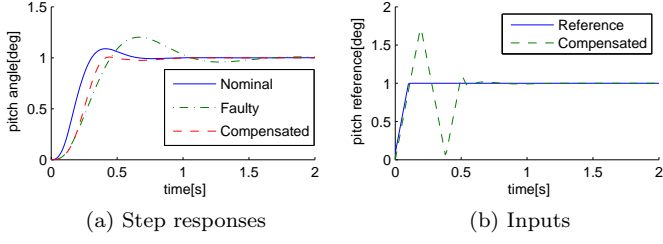


Fig. 7. Step responses of the nominal, faulty and compensated pitch system, and the corresponding inputs

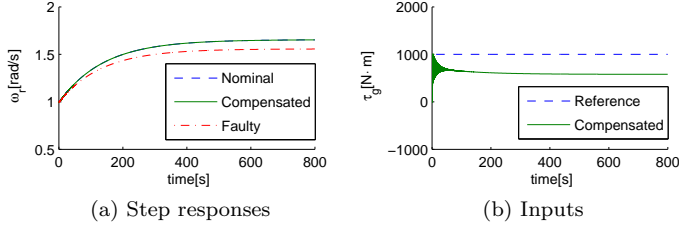
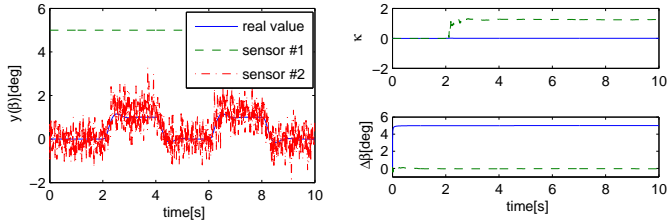


Fig. 8. Step responses of the nominal, faulty and compensated drive train system, and the corresponding inputs

and a step of 1000 N·m generator torque. In Fig. 8a, due to extra energy loss through the increased friction in fault condition, the rotor speed cannot reach the nominal value. By reducing the generator torque as compensation (Fig. 8b), which acts as resistance for the drive train in order to extract wind energy from the rotor, the response of the compensated system is almost the same as that of the nominal system (Fig. 8a).



(a) Sensor measurements (sensor 1: constant 5; sensor 2: gain 1.2) (b) Fault parameter estimation (solid: sensor 1; dashed: sensor 2)

Fig. 9. Simulation of the pitch sensor fault estimation

Fig. 9 shows the pitch system sensor fault simulation results. Both of the sensors are faulty, with sensor 1 having constant output 5 and sensor 2 gain factor 1.2 (Fig. 9a). It can be seen that the extended Kalman Filter estimates the sensor fault parameters quite well (Fig. 9b). These parameters are not directly used in the compensation. But it is crucial for correct estimation of the states, which are used in the pre-compensators. Simulation results of the drive train system are similar and will not be shown here.

#### 4.2 Nominal Condition Simulation

This simulation is to show the nominal performance of the proposed controller. The wind profile from the benchmark is used, and is compressed to 300 s. Simulation results are shown in Fig. 10 to 12. At the beginning, the low wind

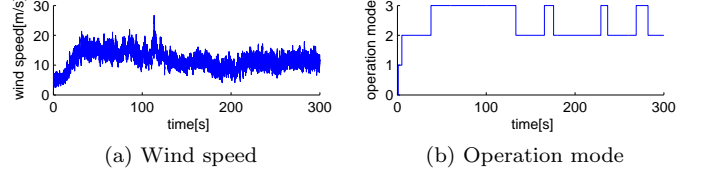


Fig. 10. Wind profile and operation mode

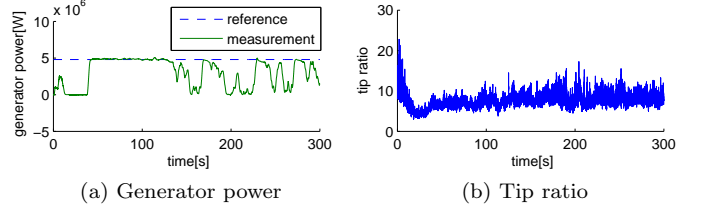


Fig. 11. Control specifications

speed leads to large tip ratio, thus a generator torque is applied correspondingly to decelerate the rotor (Fig. 12b). From around 40 s, when the wind speed increases, the wind turbine switches to operation region III. Both the pitch angle and the generator torque are manipulated, and the power measurement tracks the reference quite well (Fig. 11a). After around 130 s, the wind speed drops and the controller switches to region II, in which the tip ratio is controlled to track the optimal value ( $\lambda_{opt} = 8$ , Fig. 11b). The pitch angle keeps as 0 and the generator reference torque is manipulated (Fig. 12). It can be seen that the proposed controller controls the wind turbine quite well in the nominal condition.

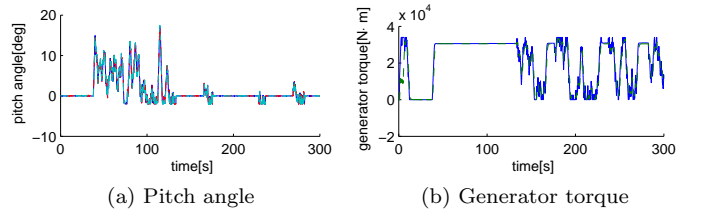


Fig. 12. Inputs to the wind turbine

#### 4.3 Monte Carlo Simulation

In order to demonstrate the fault tolerance capability of the proposed controller, Monte Carlo simulation has been done with 50 simulations. All the low and medium-severity faults occur at random times in each simulation. Comparisons between the proposed controller and the default controller provided by the benchmark are shown in Fig. 13 to 16. It can be seen that for the default controller, in certain fault cases, the tip ratio and generator power show large transients after the fault (Fig. 13a, 14a), and the input of pitch angle show large magnitude and fast movements (Fig. 15a). The generator torque also suffer from large transient in certain fault cases (Fig. 16a). It can be seen that the performance of the proposed controller in fault conditions are quite similar to that of the nominal case. No large transient occurs after fault and it uses smaller and smoother pitch angle and generator reference torque inputs (Fig. 15b, 16b).



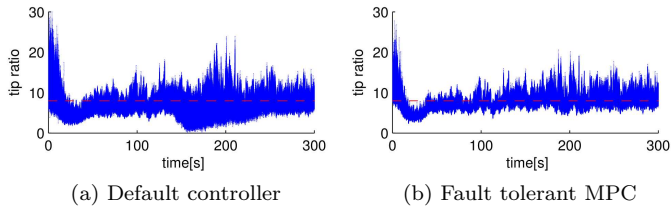


Fig. 13. Comparison of tip ratio between the proposed controller and the default one

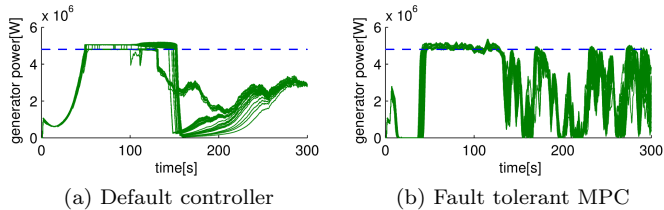


Fig. 14. Comparison of generator power between the proposed controller and the default one

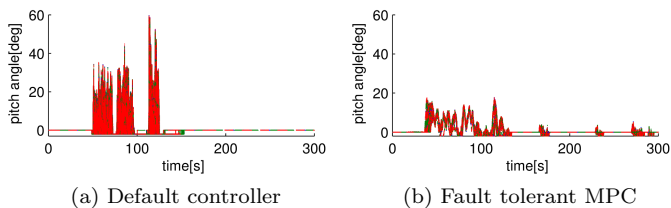


Fig. 15. Comparison of pitch reference between the proposed controller and the default one

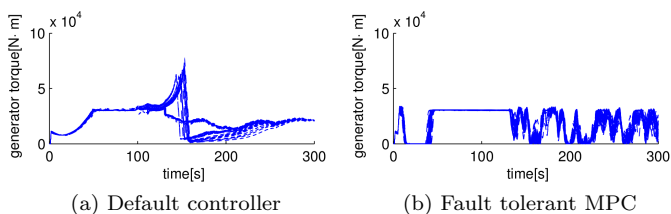


Fig. 16. Comparison of generator reference torque between the proposed controller and the default one

Statistics of the successful fault accommodation rate are shown in Table 1. For the sensor faults, the figures represents successful detection rates instead. The low successful detection rate for the pitch sensor fault is due to the fact that during some time of the simulation, the pitch angle stays as 0, which is a singular point both for the observation of sensor fault parameters and the system fault parameters. Faults happening in that period of time are not correctly estimated. But a pitch angle of 0 also means no compensation is needed, and failure in detection does not affect the controller. For the pitch actuator fault, the slow convergence rate further reduces the rate. For drive train faults, the controller accommodates quite well, but with small errors in the estimation.

Table 1. Rate of successful accommodation

Fault No.	Rate	Fault Type	Severity
1	84%	Pitch sensor fault	Low
2	98%	Pitch sensor fault	Low
3	86%	Pitch sensor fault	Low
4	100%	Drive train sensor fault	Low
5	100%	Drive train sensor fault	Low
6	0%	Pitch actuator fault	Medium
7	-	Pitch actuator fault	High
8	-	Generator system fault	High
9	100%	Drive train system fault	Medium

## 5. CONCLUSIONS

This paper proposes a fault tolerant model predictive controller for a wind turbine benchmark. The controller compensates the faults in each component with MPC pre-compensators and optimises the total performance by a global MPC. Decision and management are implemented by a supervisory controller. Simulations show the proposed controller can accommodate the system, actuator and sensor faults quite well and improves the performance over the default controller. Further work will address the investigation of fault tolerance of unexpected faults, i.e. faults that are not parameterised beforehand and thus lie outside of the predetermined classes.

## REFERENCES

- [1] C. Sloth, T. Esbensen, J. Stoustrup, Robust and Fault-Tolerant Linear Parameter-Varying Control of Wind Turbines, *Mechatronics*, vol. 21, no. 4, pp. 645-659, 2011.
- [2] E. Kamal, A. Aitouche, and M. Bayart, Fault-Tolerant Control of WECS Subject to Parametric Uncertainties and Sensor Faults, In *Control & Automation (MED), 2011 19th Mediterranean Conference on* pp. 126-131.
- [3] P. Odgaard, Fault Tolerant Control of Wind Turbines - a Benchmark Model, In *Proceedings of the 7th IFAC Symposium on Fault Detection, Supervision and Safety of Technical Processes*, pages 155-160, June 2009.
- [4] J. Maciejowski, The Implicit Daisy-Chaining Property of Constrained Predictive Control, *Applied Mathematics and Computer Science*, vol. 8, no. 4, pp. 101-117, 1998.
- [5] K. E. Johnson, L. Y. Pao, M. J. Balas, and L. J. Fingersh, Control of Variable-Speed Wind Turbines: Standard and Adaptive Techniques for Maximizing Energy Capture, *IEEE Control Systems Magazine*, vol. 26, pp. 70-81, Jun. 2006.
- [6] Fernando D. Bianchi, Hernán De Battista, and Ricardo J. Mantz. *Wind Turbine Control Systems*. Springer London, 2007.
- [7] M. Blanke, M. Staroswiecki and N.E. Wu, Concepts and Methods in Fault-Tolerant Control, In *Proceedings of the 2001 American Control Conference*, vol. 4, pp. 2606-2620.
- [8] X. Yang, Fault Tolerant Model Predictive Control of a Wind Turbine Benchmark, *First Year Report*, CUED, 2011. [http://www-control.eng.cam.ac.uk/~xy248/FYP\\_Xiaoke.pdf](http://www-control.eng.cam.ac.uk/~xy248/FYP_Xiaoke.pdf)
- [9] D. Ariens, B. Houska, H. Ferreau, and F. Logist. *ACADO for Matlab User's Manual*. 1.0beta edition, May 2010. <http://www.acadotoolkit.org/>.